Acta Oncologica, 2010; 49: 972–977

informa
healthcare

ORIGINAL ARTICLE

Adaptive radiotherapy based on contrast enhanced cone beam CT imaging

ÅSTE SØVIK[1,2], JAN RØDAL[2,3], HEGE K. SKOGMO[1], CHRISTOFFER LERVÅG[2], KARSTEN EILERTSEN[2] & EIRIK MALINEN[2]

[1]*Department of Companion Animal Clinical Sciences, Norwegian School of Veterinary Science, Oslo, Norway,*
[2]*Department of Medical Physics, The Norwegian Radium Hospital, Oslo University Hospital, Oslo, Norway and*
[3]*Department of Physics, The Norwegian University of Science and Technology, Trondheim, Norway*

Abstract

Cone beam CT (CBCT) imaging has become an integral part of radiation therapy, with images typically used for offline or online patient setup corrections based on bony anatomy co-registration. Ideally, the co-registration should be based on tumor localization. However, soft tissue contrast in CBCT images may be limited. In the present work, contrast enhanced CBCT (CECBCT) images were used for tumor visualization and treatment adaptation. *Material and methods.* A spontaneous canine maxillary tumor was subjected to repeated cone beam CT imaging during fractionated radiotherapy (10 fractions in total). At five of the treatment fractions, CECBCT images, employing an iodinated contrast agent, were acquired, as well as pre-contrast CBCT images. The tumor was clearly visible in post-contrast minus pre-contrast subtraction images, and these contrast images were used to delineate gross tumor volumes. IMRT dose plans were subsequently generated. Four different strategies were explored: 1) fully adapted planning based on each CECBCT image series, 2) planning based on images acquired at the first treatment fraction and patient repositioning following bony anatomy co-registration, 3) as for 2), but with patient repositioning based on co-registering contrast images, and 4) a strategy with no patient repositioning or treatment adaptation. The equivalent uniform dose (EUD) and tumor control probability (TCP) calculations to estimate treatment outcome for each strategy. *Results*. Similar translation vectors were found when bony anatomy and contrast enhancement co-registration were compared. Strategy 1 gave EUDs closest to the prescription dose and the highest TCP. Strategies 2 and 3 gave EUDs and TCPs close to that of strategy 1, with strategy 3 being slightly better than strategy 2. Even greater benefits from strategies 1 and 3 are expected with increasing tumor movement or deformation during treatment. The non-adaptive strategy 4 was clearly inferior to all three adaptive strategies. *Conclusion*. CECBCT may prove useful for adaptive radiotherapy.

With the advent of intensity modulated radiotherapy, highly conformal radiation doses can be delivered to the tumor or tumor sub-volumes [1]. However, inaccuracies in patient setup and/or changes in patient anatomy during treatment may reduce the target coverage and lead to increased dose in adjacent normal tissue structures. Hence, techniques for monitoring both changes in the extent and localization of the tumor during treatment are needed to ensure optimal treatment outcome of conformal radiotherapy [2].

Cone beam CT (CBCT) imaging has become an integral part of external beam radiation therapy, and offers an attractive monitoring option, as the necessary equipment is already available in the treatment room and images are acquired in the treatment position [3,4]. At present, the images are typically used for patient setup corrections, either based on bony anatomy landmarks or soft tissue structures, including the tumor itself [5,6]. However, CBCT may not produce images with sufficient soft tissue contrast for tumor localization in all treatment sites [7,8]. Hence, contrast enhanced CBCT (CE-CBCT) imaging with iodinated contrast agents have been proposed in order to increase soft tissue contrast [5,7,9].

The use of CBCT in adaptive radiotherapy, where a target volume definition is based on the CBCT

Correspondence: Åste Søvik, Department of Companion Animal Clinical Sciences, Norwegian School of Veterinary Science, Post Box 8146 Dep 0033 Oslo, Norway. Tel: +47 22964957. E-mail: aste.sovik@nvh.no

(Received 19 May 2010; accepted 27 May 2010)

ISSN 0284-186X print/ISSN 1651-226X online © 2010 Informa Healthcare
DOI: 10.3109/0284186X.2010.498433

images and used to generate a "plan of the day", has been suggested [10,11]. Here, both interfraction tumor movement and changes in size and shape can be taken into account. When using iodinated contrast agents, increased contrast between tumor and normal tissues may also aid target volume definition. Moreover, a boost volume consisting of the contrast enhancing region could be defined, making biological image-guided dose escalation based on CBCT feasible.

The aim of the present work was to explore the potential role of contrast-enhanced cone beam CT in tumor-guided adaptive radiotherapy. Contrast-enhanced CBCT images acquired during the course of fractionated radiotherapy of a spontaneous canine maxillary tumor were used as a basis for treatment planning according to four different treatment strategies, ranging from no adaptation during treatment to a fully adaptive strategy. The resulting dose plans were evaluated in terms of the expected treatment outcome, as described by the equivalent uniform dose (EUD) and the tumor control probability (TCP).

Material and methods

Radiotherapy and imaging

A nine-year-old female border collie with a 14 cm^3 spontaneous right maxillary round cell tumor was treated with intensity modulated radiotherapy (IMRT) with 6 MV photons to a total dose of 40 Gy delivered in 10 fractions at an Elekta Synergy linear accelerator (Elekta AB, Stockholm, Sweden) equipped with a CBCT system (XVI). The patient was placed in prone position on a vacuum cushion (VacFix, Par Scientific A/S, Odense Denmark) in a polymethyl methacrylate (PMMA) case, and the upper jaw was fixed by a dental form anchored to the PMMA case.

CBCT imaging was performed prior to each treatment fraction, and automatic bone matching to the reference CT images acquired three days before the start of therapy was used to correct patient set-up. At five of the treatment sessions (1, 3, 5, 7, and 10), contrast-enhanced CBCT images were obtained in addition to the standard CBCT images. The contrast-enhanced images were acquired one minute after manual injection of 600 mg/kg iohexol (Omnipaque 300 mg I/ml, GE Healthcare, Oslo, Norway), and no repositioning was allowed between pre- and post-contrast scans.

All imaging and treatments were performed under general anesthesia with continuous rate infusion of propofol 10 mg/kg/h (PropoVet, Abbot, Illinois, USA), after premedication with medetomidine 5 μg/kg iv (Domitor vet., Orion, Turku, Finland) and butorfanol 0.05 mg/kg iv (Dolorex vet., Intervet, Boxmeer, the Netherlands) and induction of anesthesia with propofol 2 mg/kg iv. The patient was intubated during anesthesia and oxygen supplemented via the tube at a flow rate of 2 l/min. The study was approved by the National Animal Research Authority and written informed consent was obtained from the owner. The treatment was performed with curative intent.

Image analysis

Coronal CBCT images with voxel dimensions $1 \times 1 \times 1$ mm were reconstructed from the volumetric uptakes. Contrast-enhancement images were created through subtraction of pre-contrast from post-contrast images. The subtraction images were normalized to normal tissue enhancement at the first treatment session to correct for variations in injection time due to manual injection. Images were then scaled with a window center of 100 Hounsfield units (HU) and a window width of 100 HU, as this was found to give optimal visualization of the tumor for tumor contouring (see below). The scaled contrast enhancement images were given DICOM headers using Ruby DICOM (http://dicom.rubyforge.org/), so that the images could be exported to the treatment planning system (see below) Analysis of the reconstructed images was performed using custom written software in IDL 6.2 (ITT Visual Information Solutions, Boulder, USA).

Treatment planning and adaptive strategies

The pre-contrast CBCT images and contrast enhancement images for fraction 1, 3, 5, 7, and 10 were transferred to the VSIM virtual simulator (v2.2, Siemens Medical Solutions, Inc., Malvern, USA). For each image series, the gross tumor volume (GTV) was contoured manually in pre-contrast CBCT images guided by the contrast enhancement images in overlay mode. A planning target volume (PTV) was automatically generated by adding a 5 mm isotropic margin to the GTV. IMRT dose planning with seven fields and 6 MV photons was performed in the KonRad planning system (v2.2.18, Siemens Medical Solutions, Inc., Malvern, USA). A simultaneous integrated boost was adopted, prescribing a dose of 4.0 Gy per fraction for 10 fractions to the PTV, while the CE-CBCT GTV was given a dose of 4.6 Gy per fraction.

Four different treatment strategies were investigated. In the first, fully adaptive strategy, new radiotherapy target structures were created for each CE-CBCT image set and replanning was performed based on these target structures. In the second strategy, dose planning was done only based on CE-CBCT images acquired at the first treatment session, but patient repositioning based on bony anatomy

co-registration was performed for each treatment fraction. For co-registration in 3D, bone was segmented from the image series and translation vectors were obtained by optimizing the correlation between the segmented images using a modified version of a fast Fourier transform algorithm published previously [12]. Rotations were not included in the co-registration. In the third strategy, dose planning was only conducted based on the CE-CBCT images from the first treatment session as well, but the patient repositioning was guided by co-registration of the contrast-enhancement matrices using the Fourier algorithm given above. The fourth strategy was non-adaptive, with dose planning based on the CE-CBCT images from the first treatment session and no patient repositioning at the following treatment fractions.

Outcome modeling

The resulting dose distributions in the GTV were evaluated in terms of the equivalent uniform dose and the expected tumor control probability (TCP). The EUD was calculated according to the mechanistic model of Niemierko [13], where the EUD satisfies the following condition:

$$SF = e^{-n(aEUD+\beta EUD^2)} = \frac{1}{N}\sum_i e^{-n(ad_i+\beta d_i^2)} \quad (1)$$

Here, SF is the fraction of surviving clonogens, n is the number of treatment fractions, N is the number of voxels, d_i is the dose given to voxel i, and α and β are the linear and quadratic cell inactivation coefficients, respectively. Tumor control probability was calculated by use of the linear quadratic cell survival model [14], according to:

$$TCP = e^{-\rho V\prod_{j=1}^{10} SF_j} \quad (2)$$

where j is the treatment fraction, ρ the clonogen density in the tumor and V the tumor volume. Interpatient variations in the intrinsic radiosensitivity α was taken into account by convolving Equation 2 with a Gaussian standard deviation of σ_α. The following radiobiological parameters were used in the calculations: $\alpha = 0.3$ Gy^{-1}, $\beta = 0.03$ Gy^{-2}, $\rho = 10^7$, and $\sigma_\alpha = 0.07$ [14]. Radiation sensitivity and clonogen density were assumed to be constant in the GTV. For the treatment fractions where no CE-CBCT images were available, the GTVs created on the previous treatment fractions were used.

Results

Contrast-enhancement images (color wash) overlaid on pre-contrast cone beam CT images (grayscale) for treatment sessions 1, 3, 5, 7, and 10 are shown in Figure 1. The tumor contour (GTV) for each image set is shown in blue. The tumor was clearly visualized in the contrast-enhanced overlays for all CE-CBCT image series. In contrast, tumor boundaries could not be accurately determined in the pre-contrast CBCT images (data not shown).

Figure 2 shows the IMRT dose plan created based on the contrast-enhancement overlay images from treatment session 1. The contour of the CE-CBCT-based GTV, with a prescription dose of 46 Gy, is shown in blue, and the PTV, with prescribed dose 40 Gy, is shown in pink.

In Figure 3, image co-registration based on either bone matching (upper row) or contrast enhancement matching (lower row) is illustrated. Both methods were seen to provide appropriate matching, as the delineated tumor contours in both cases showed maximal overlap after co-registration. The corresponding patient repositioning translation vectors for all five treatment sessions for which CE-CBCT was performed is shown in Table I. The image set from treatment session 1 was taken as the reference images, and the translation vector was consequently [0, 0, 0]

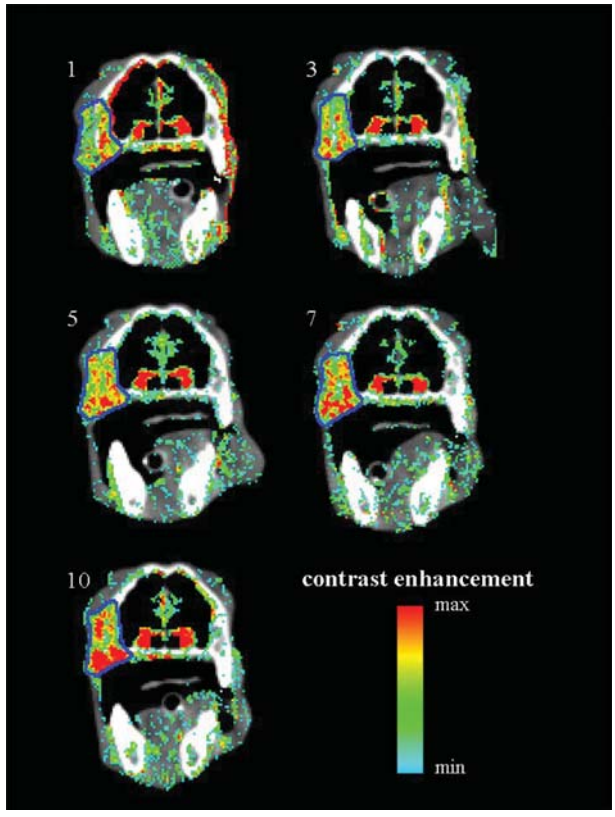

Figure 1. Pre-contrast cone beam CT images (grayscale) overlaid with contrast enhancement images (post-contras minus pre-contrast, color wash) for the five treatment sessions for which contrast-enhanced cone beam CT was performed (fractions 1, 3, 5, 7, and 10). The tumor contour for each image set is shown in blue.

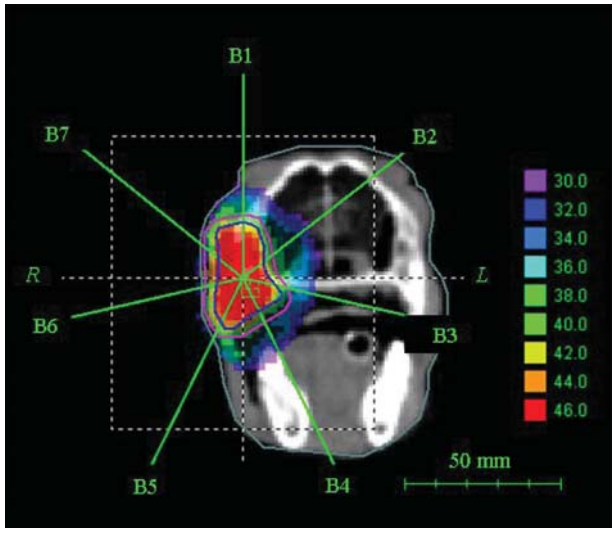

Figure 2. The IMRT dose plan for treatment fraction 1. The GTV is shown in blue and the PTV in pink. The prescribed dose to the GTV was 46 Gy and the prescribed dose to the PTV 40 Gy.

for this session. Good agreement between the translation vectors resulting from bone matching and matching on the contrast-enhancement matrices was found, with translation vectors being either identical or within 1 mm of each other in each direction.

The EUD for each treatment strategy and treatment session is shown in Figure 4. The fully adaptive strategy was seen to give the highest EUDs, followed by the strategy where the patient was repositioned based on co-registration of contrast-enhancement images and the strategy where the patient was repositioned based on co-registration of bony anatomy. The non-adaptive strategy with no patient repositioning resulted in the lowest EUDs. In particular, for treatment fraction 3, where the greatest patient translation was required (see Table I), the non-adaptive strategy was clearly inferior to the three other strategies. The tumor control probability associated with the different strategies was 0.56 for the fully adaptive one, 0.55 for both patient repositioning based on bony anatomy and on contrast-enhancement, and 0.50 for no adaptation or repositioning.

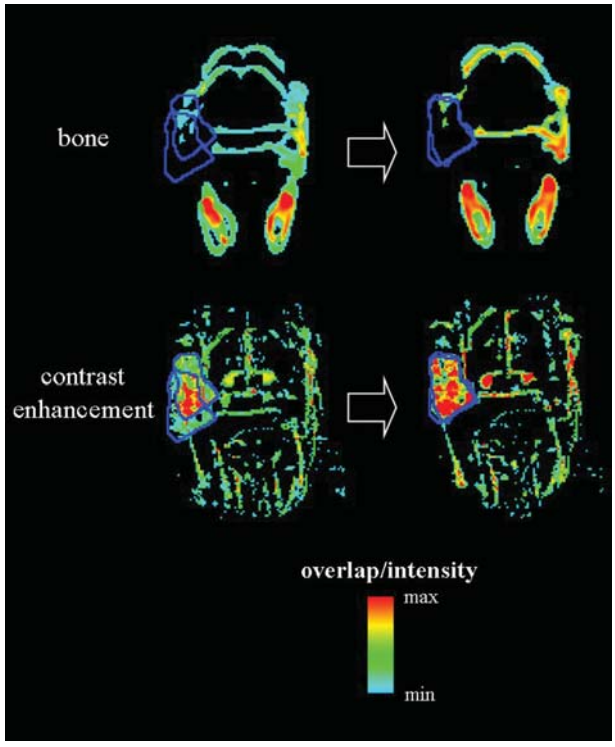

Figure 3. Patient repositioning based on co-registering bony anatomy (upper row) and contrast enhancement (lower row). Cone beam CT images and contrast enhancement images from treatment session 3 are matched to their respective images taken at treatment session 1. The tumor contour is shown in blue.

Discussion

In the present work, the potential of contrast-enhanced cone beam CT for treatment adaptation was explored. The tumor was clearly discriminated from normal tissue in the contrast enhancement images. Treatment adaptation based on serial CE-CBCT images, both in the form of replanning and patient repositioning, was investigated and compared both to patient repositioning based on conventional CBCT images (bony anatomy matching) and no treatment adaptation. In the present case, where the tumor was localized in bone, a high correlation between patient repositioning vectors based on matching the contrast-enhancement and the bony anatomy was found. Furthermore, the expected treatment outcomes for the three different adaptive strategies (i.e. replanning at each treatment session where CE-CBCT images were available and patient repositioning based on matching of contrast-enhancement or bony anatomy) were similar. However, for soft tissue tumors showing, both changes in tumor position relative to bone and greater deformation in the size of the tumor during radiation therapy may occur [15], a greater benefit from adaptive strategies based on CE-CBCT imaging is expected.

Table I. Translation vectors for patient repositioning following bone and contrast-enhancement (CE) matching of cone beam CT images

	X direction (mm)		Y direction (mm)		Z direction (mm)	
Fraction #	Bone	CE	Bone	CE	Bone	CE
1	0	0	0	0	0	0
3	2	2	9	9	2	2
5	−3	−3	2	2	1	1
7	−1	0	2	1	2	2
10	−2	−3	3	4	0	1

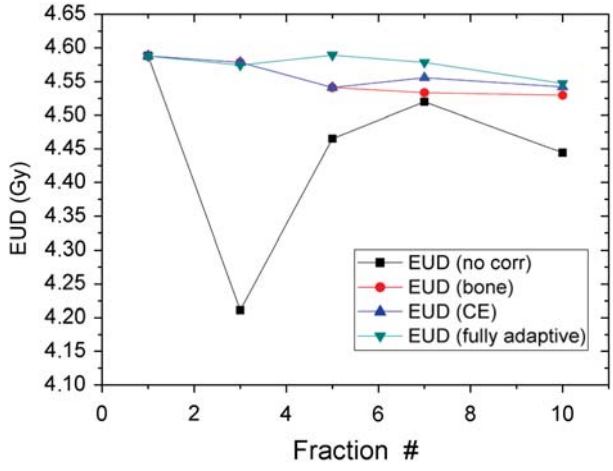

Figure 4. Equivalent uniform dose (EUD) for the dose distributions resulting from the four different treatment strategies; fully adaptive (green), patient repositioning based on matching of contrast enhancement matrices (blue), patient repositioning based on matching of bony anatomy (red) and no repositioning or treatment adaptation (black).

In the present work, imaging was performed under general anesthesia, which ensured patient immobility both during CBCT imaging and between pre- and post-contrast imaging. When applied to the non-anesthetized patient, adequate patient fixation should be ensured. Motion of the patient between pre- and post-contrast imaging can be detected as edge artifacts in the contrast enhancement subtraction images, particularly at bone/air and skin/air interfaces. This can be seen in Figure 1 for treatment session 1, where a slight shift of the patient occurred during anesthetic monitoring between pre- and post-contrast images.

Contrast-enhanced CBCT imaging was performed approximately every second treatment session in the present study. As subtraction images were used to visualize the contrast-enhancement, each CE-CBCT scan gave an additional radiation dose to the patient [16]. Furthermore, when intravenous iodinated contrast agents are employed repeatedly, the potential for contrast-agent induced toxicity, such as nephrotoxicity, must be considered [17]. Hence, repeated CE-CBCT scans may not be appropriate for patients with pre-existing renal insuffiency, and periprocedural hydration and the use of non-ionic contrast media of low osmolarity could be considered to minimize the risk of contrast agent induced nephrotoxicity [17]. Novel contrast agent formulations that provide longer lasting contrast enhancement in the tumor are being developed [18] and may allow daily CE-CBCT imaging at a decreased risk of nephrotoxicity. In the current canine case, a non-ionic low osmolarity contrast agent was used and intravenous fluids were available as a part of the anesthetic protocol. Furthermore, a full biochemical blood profile was obtained both prior to and after radiotherapy, and no adverse effects on kidney function of the contrast agent administration were detected.

In the present work, the CE-CBCT target structures were contoured manually, and these target structures were taken to represent the "true" tumor volume in the treatment outcome calculation. Alternatively, automatic target volume segmentation based on the CT images could be employed to standardize the target volume definitions [19]. Furthermore, as the fully adaptive strategy depends on replanning several times during treatment, steps must be taken to ensure that each treatment plan is of optimal quality.

Dose escalation, in terms of a simultaneous integrated boost, was explored in the current study, and the GTV derived from CE-CBCT was tentatively given 15% higher dose than the PTV, as a higher clonogen density is expected in the GTV. Parameters from dynamic analysis of CT images have been shown to correlate to tumor microenvironmental factors that may influence the response to radiotherapy [20]. However, the increased scan time in CBCT imaging precludes the use of dynamic analysis for this modality. Hence, if dose escalation is to be performed based on CE-CBCT imaging, dose escalation factors must be chosen ad hoc, and further work is needed to characterize the relationship between CT contrast enhancement and treatment response [21].

Most studies on biological image-guided treatment planning have focused on positron emission tomography (PET) or magnetic resonance (MR) imaging [22]. Both these imaging modalities are expected to offer increased tumor biological information over CE-CBCT. However, disadvantages with PET or MR images are that they are acquired outside the treatment room and that frequent imaging during the course of treatment is not feasible. Moreover, a high positioning accuracy may be necessary to retain the advantage of biological-image guided dose escalation using these modalities [23]. In this case, CE-CBCT could play a role in the daily localization of the target volume. However, validation of CE-CBCT target structures against other tumor imaging modalities and pathological specimens are needed and such validation is the subject of our current research.

Conclusions

Treatment adaptation, both in the form of replanning and patient repositioning, based on contrast-enhanced cone beam CT images is feasible and may lead to improved treatment outcome. However, further work is needed to describe the patient sub-population

expected to benefit from this form of treatment adaptation and to define optimal imaging schedules and adaptation strategies.

Acknowledgements

This work was supported by the Norwegian Cancer Society. Approval by National Animal Research Authority: Registration number 09/36890-1, issued 15.04.2009.

Declaration of interest: The authors report no conflicts of interest. The authors alone are responsible for the content and writing of the paper

References

[1] Intensity Modulated Radiation Therapy Collaborative Work Group. Intensity-modulated radiotherapy: Current status and issues of interest. Int J Radiat Oncol Biol Phys 2001; 51:880–914.

[2] Grau C, Muren LP, Hoyer M, Lindegaard J, Overgaard J. Image-guided adaptive radiotherapy - integration of biology and technology to improve clinical outcome. Acta Oncol 2008;47:1182–5.

[3] Jaffray DA, Siewerdsen JH, Wong JW, Martinez AA. Flat-panel cone-beam computed tomography for image-guided radiation therapy. Int J Radiat Oncol Biol Phys 2002;53: 1337–49.

[4] Verellen D, De RM, Tournel K, et al. An overview of volumetric imaging technologies and their quality assurance for IGRT. Acta Oncol 2008;47:1271–8.

[5] Jaffray DA. Kilovoltage volumetric imaging in the treatment room. Front Radiat Ther Oncol 2007;40:116–31.

[6] Moore CJ, Amer A, Marchant T, et al. Developments in and experience of kilovoltage X-ray cone beam image-guided radiotherapy. Br J Radiol 2006;79 Spec No 1:S66–S78.

[7] Higgins J, Bezjak A, Franks K, et al. Comparison of spine, carina, and tumor as registration landmarks for volumetric image-guided lung radiotherapy. Int J Radiat Oncol Biol Phys 2009;73:1404–13.

[8] McBain CA, Henry AM, Sykes J, et al. X-ray volumetric imaging in image-guided radiotherapy: The new standard in on-treatment imaging. Int J Radiat Oncol Biol Phys 2006; 64:625–34.

[9] Igaki H, Nakagawa K, Yamashita H, et al. Contrast media-assisted visualization of brain metastases by kilovoltage cone-beam CT. Acta Oncol 2009;48:314–7.

[10] Jaffray D, Kupelian P, Djemil T, Macklis RM. Review of image-guided radiation therapy. Expert Rev Anticancer Ther 2007;7:89–103.

[11] Tanyi JA, Fuss MH. Volumetric image-guidance: Does routine usage prompt adaptive re-planning? An institutional review. Acta Oncol 2008;47:1444–53.

[12] Eilertsen K, Skretting A, Tennvassas TL. Methods for fully automated verification of patient set-up in external beam radiotherapy with polygon shaped fields. Phys Med Biol 1994;39:993–1012.

[13] Niemierko A. Reporting and analyzing dose distributions: A concept of equivalent uniform dose. Med Phys 1997; 24:103–10.

[14] Nahum AE, Sanchez-Nieto B. Tumor control probability modelling: Basic principles and applications in treatment planning. Physica Medica 2001;XVII:13–23.

[15] Dawson LA, Sharpe MB. Image-guided radiotherapy: Rationale, benefits, and limitations. Lancet Oncol 2006;7:848–58.

[16] Perks JR, Lehmann J, Chen AM, Yang CC, Stern RL, Purdy JA. Comparison of peripheral dose from image-guided radiation therapy (IGRT) using kV cone beam CT to intensity-modulated radiation therapy (IMRT). Radiother Oncol 2008;89:304–10.

[17] Hasebroock KM, Serkova NJ. Toxicity of MRI and CT contrast agents. Expert Opin Drug Metab Toxicol 2009;5:403–16.

[18] Zheng J, Liu J, Dunne M, Jaffray DA, Allen C. In vivo performance of a liposomal vascular contrast agent for CT and MR-based image guidance applications. Pharm Res 2007;24:1193–201.

[19] Soler L, Delingette H, Malandain G, et al. Fully automatic anatomical, pathological, and functional segmentation from CT scans for hepatic surgery. Comput Aided Surg 2001;6:131–42.

[20] Haider MA, Milosevic M, Fyles A, et al. Assessment of the tumor microenvironment in cervix cancer using dynamic contrast enhanced CT, interstitial fluid pressure and oxygen measurements. Int J Radiat Oncol Biol Phys 2005;62:1100–7.

[21] Greco C, Clifton LC. Broadening the scope of image-guided radiotherapy (IGRT). Acta Oncol 2008;47:1193–200.

[22] Søvik Å, Malinen E, Olsen DR. Strategies for biologic image-guided dose escalation: A review. Int J Radiat Oncol Biol Phys 2009;73:650–8.

[23] Søvik Å, Malinen E, Skogmo HK, Bentzen SM, Bruland ØS, Olsen DR. Radiotherapy adapted to spatial and temporal variability in tumor hypoxia. Int J Radiat Oncol Biol Phys 2007;68:1496–504.